A Multi-Objective Evolutionary Approach for Linear Antenna Array Design and Synthesis

Subhrajit Roy*, Saúl Zapotecas Martínez†, Carlos A. Coello Coello‡ and Soumyadip Sengupta§

*§Jadavpur University, Dept. of Electronics and Telecommunication Engineering,
Kolkata 700 032, INDIA
†‡CINVESTAV-IPN (Evolutionary Computation Group),
Departamento de Computación, México D.F. 07360, MÉXICO
Email: *roy.subhrajit20@gmail.com, †saul.zapotecas@gmail.com,
‡ccoello@cs.cinvestav.mx, §roni14may@gmail.com

***Abstract*—The linear antenna array design problem is one of the most important in electromagnetism. While designing a linear antenna array, the goal of the designer is to achieve the "minimum average side lobe level" and a "null control" in specific directions. In contrast to the existing methods that attempt to minimize a weighted sum of these two objectives considered here, in this paper our contribution is twofold. First, we have considered these as two distinct objectives which are optimized simultaneously in a multi-objective framework. Second, for directivity purposes, we have introduced another objective called the "maximum side lobe level" in the design formulation. The resulting multi-objective optimization problem is solved by using the recently-proposed decomposition-based Multi-Objective Particle Swarm Optimizer (dMOPSO). Our experimental results indicate that the proposed approach is able to obtain results which are better than those obtained by two other state-of-the-art Multi-Objective Evolutionary Algorithms (MOEAs). Additionally, the individual minima reached by dMOPSO outperform those achieved by two single-objective evolutionary algorithms.**

I. Introduction

Antenna arrays play an important role in detecting and processing signals arriving from different directions. Nowadays, antenna arrays are preferred because the use of a single element has several limitations in terms of directivity and bandwidth. Antenna arrays overcome such defects by associating each antenna element to different electrical and geometrical configurations, so that it can have its beam-pattern modified with an amplitude and phase distribution called the weights of the array. After post-processing the antenna outputs, the signals are weighted and summed to give the antenna array beam-pattern. On the other hand, the antenna array pattern synthesis problem consists of finding weights that satisfy a set of specifications on the beam pattern. Antenna arrays have found several applications in radar, sonar, radio, and third generation wireless communication systems [4, 7, 20].

The main goal in the design of an antenna array structure is to find the positions of the array elements that produce a radiation pattern as a whole that closely matches the desired pattern [19]. Recently, the synthesis of linear array elements separated in a non-linear fashion has become immensely popular among researchers working in electromagnetism. Current mathematical programming techniques are not able to satisfy researchers due to their limitations, including the fact that most of them are likely to get trapped in local optimal points and are highly sensitive to the initial search point. For this reason, several researchers have opted for the use of metaheuristics (mainly, evolutionary algorithms) to reduce the Side Lobe Levels (SLLs) and the Null Control (NC) from the designed arrays (see for example [2, 3, 12, 21, 22]). Such techniques are a suitable alternative to the conventional methods because of their ability to deal with difficult problems featuring complex landscapes. Most of these approaches tackle the objectives simultaneously creating a single objective function by taking a weighted sum of the objective functions. Clearly, when using such a weighted sum method, the solution obtained will depend on the values of the specified weights, and determining such weights is not an easy task.

Motivated by the inherent multi-objective nature of the linear antenna design problem and to avoid the problems associated with the use of weighted sum approaches, in this paper, we present a multi-objective formulation of the problem of our interest and we adopt a recent approach called decomposition-based Multi-Objective Particle Swarm Optimizer (dMOPSO) for solving it. In contrast to the plethora of works which consider only the average SLL and NC as the objective functions, we consider here an additional objective (maximum SLL) in order to increase the overall directivity of the antenna array. As we will see later in this paper, the solutions obtained by dMOPSO outperform those obtained by two other state-of-the-art multi-objective evolutionary algorithms (MOEAs). Additionally, the individual minima obtained by dMOPSO also outperform those obtained by two single-objective evolutionary algorithms reported in the specialized literature.

The remainder of this paper is organized as follows. Section II provides the basic concepts adopted in this paper, as well as the multi-objective formulation of the problem of our interest. In Section III, we provide a short description of the multi-objective particle swarm optimizer adopted in this work. Section IV shows the results obtained in our experimental study. In Section V, we give a brief discussion

of the results obtained. Finally, in Section VI, we provide our conclusions and some possible paths for future research.

II. Basic Concepts and Problem Formulation

A. Notions of Multi-Objective Optimization

An unconstrained multi-objective optimization problem (MOP), can be stated as follows [1]:

$$\min_{x \in \Omega} \quad \{F(x)\} \tag{1}$$

where Ω defines the search space and F is defined as the vector of the objective functions:

$$F : \Omega \to \mathbb{R}^k, \quad F(x) = (f_1(x), \ldots, f_k(x))^T$$

where $f_i : \mathbb{R}^n \to \mathbb{R}$ is an unconstrained function.

In multi-objective optimization, it is desirable to produce a set of trade-off solutions representing the best possible compromises among the objectives (i.e., solutions such that no objective can be improved without worsening another). In order to describe the concept of optimality in which we are interested, the following definitions are introduced [14].

Definition 1. Let $x, y \in \Omega$; we say that x *dominates* y (denoted by $x \prec y$) if and only if, $f_i(x) \leq f_i(y)$ and $F(x) \neq F(y)$.

Definition 2. Let $x^\star \in \Omega$; we say that $x^\star$ is a *Pareto optimal* solution, if there is no other solution $y \in \Omega$ such that $y \prec x^\star$.

Definition 3. The *Pareto Optimal Set* $\mathcal{PS}$ is defined by:

$$\mathcal{PS} = \{x \in \Omega | x \text{ is Pareto optimal solution}\}$$

Definition 4. The *Pareto Optimal Front* $\mathcal{PF}$ is defined by:

$$\mathcal{PF} = \{F(x) | x \in \mathcal{PS}\}$$

The main goal of a MOEA is to generate as many (different) elements of the Pareto optimal set as possible, while maintaining a distribution of solutions as uniform as possible along the Pareto front.

B. Multi-Objective Formulation of the Problem

An antenna array is a configuration of individual radiating elements that are arranged in an space and can be used to produce a directional radiation pattern. For a linear antenna array, let us assume that we have $2N$ isotropic radiators placed symmetrically along the z-axis (the array geometry is shown in Fig. 1). The array factor in the azimuth plane can be written as:

$$AF(\phi) = 2 \sum_{n=1}^{N} I_n \cos\left[k \cdot z_n \cdot \cos(\phi) + \varphi_n\right] \tag{2}$$

where I_n is the excitation amplitude, $k = \frac{2\pi}{\lambda}$ is the wave number, z_n is the location of the z-th element, φ_n defines the phase and ϕ represents the angle measured from the array line.

[1]Without loss of generality, we assume minimization

Assuming an uniform excitation of amplitude and phase (i.e. $I_n = 1$ and $\varphi_n = 0$ for all the elements), the array factor can be written as:

$$AF(\phi) = 2 \sum_{n=1}^{N} I_n \cos\left[k \cdot z_n \cdot \cos(\phi)\right] \tag{3}$$

The main goal of the optimizer is to find the locations z_n of the array elements that will result in an array beam with minimum Side Lobe Level (SLL) and nulls at specific directions but subject to certain constraints. In an antenna array, if the adjacent elements are located very near, then that can lead to mutual coupling effects. On the other hand, if they are located very far, then, occurrence of grating lobes can take place. Therefore, the distance among adjacent elements needs to be constrained. The constraints which are considered for normalizing the element spacing z_n is given by:

$$0.5 \leq z_{n+1} - z_n \leq 1, n \in [1, N-1]$$

The first element along the positive z-axis needs to be placed such that it is neither too close nor too far from the first element on the negative z-axis. Therefore, the constraint for the first element is given by:

$$0.3 \leq z_1 \leq 0.5$$

In contrast with most of the design formulations of antenna arrays which consider only the Average Side Lobe Level (ASLL)–see for example [5, 17], we consider here an additional objective function for the side lobe suppression: the Maximum Side Lobe Level (MSLL). This objective function is considered for directivity purposes. The directivity of an antenna array is an important parameter to be considered during the design stage, since the design is considered to be more efficient if the directivity is increased. In this study, besides the ASLL reduction we have also given special emphasis on reducing the two maximum lobes: the adjacent lobe on the *left side* ($MSSL1$) and the adjacent lobe on the *right side* ($MSLL2$). This ensures that the energy contents is mostly confined to the maximum lobe, thereby increasing the directivity of the entire array. Then, the two cost functions (i.e., ASLL and MSLL) to be minimized are mathematically stated as:

$$f_{ASLL} = \sum_i \frac{1}{\Delta\phi_i} \int_{\phi_{li}}^{\phi_{ui}} |AF(\phi)|^2 d\phi \tag{4}$$

$$f_{MSLL} = |AF(\phi_{MSLL1})| + |AF(\phi_{MSLL2})| \tag{5}$$

where $MSLL1$ and $MSLL2$ are two lobes by the side of the MSLL.

As these two objective functions are not conflicting, a weighted sum of these objectives could be taken. Therefore, we define the overall objective function for the side lobe suppression f_{SLL} as a weighted sum of the above objectives, denoted by:

$$f_{SLL} = \alpha \cdot f_{SLA} + \beta \cdot f_{MSL} \tag{6}$$

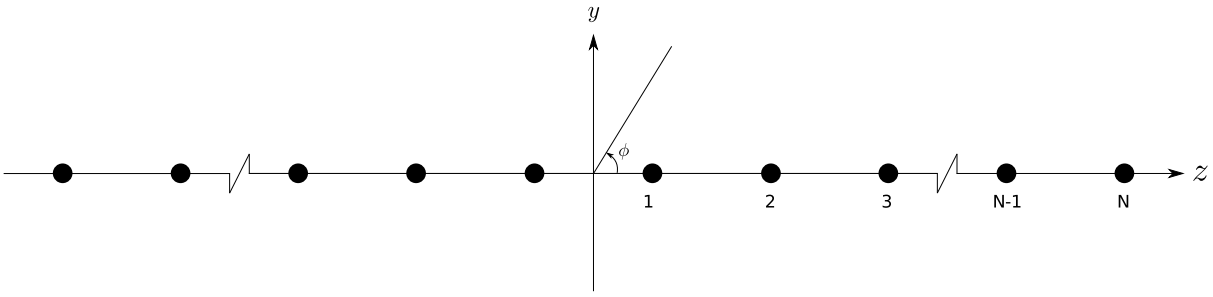

Fig. 1. Symmetrically placed linear array.

where $\alpha = 0.2$ and $\beta = 0.1$, and the null control f_{NC} is defined as:

$$f_{NC} = \sum_{k} |AF(\phi_k)|^2 \tag{7}$$

In this way, equations (6) and (7) are considered as two distinct objectives that are simultaneously optimized in a multi-objective framework. A MOEA will allow us to find out the right balance between the two above objective functions. When a MOEA is used, we obtain a set of solution which represent the best compromises among such objectives. Therefore, a MOEA will allow us greater flexibility in designing a linear antenna array than single-objective evolutionary approaches, which provide only one optimal solution per run, which might not completely satisfy the designer's needs.

III. The Multi-Objective Particle Swarm Optimizer

A Pareto optimal solution to a MOP, under some mild assumptions, can be an optimal solution to a scalar optimization problem in which the objective is an aggregation of all the objective functions f_i's. Therefore, an approximation of the Pareto optimal front can be achieved by decomposing a MOP into several single-objective optimization problems. This is the main motivation behind current decomposition-based MOEAs [15, 18, 23, 24].

Recently, Zapotecas and Coello [23] proposed a novel decomposition-based Multi-Objective Particle Swarm Optimizer (dMOPSO). This MOEA employs a decomposition framework similar to the one adopted by MOEA/D [24]. However, a $(\mu + \lambda)$-selection mechanism (selecting the best solution to each subproblem) is employed instead of a mechanism to update a neighborhood as adopted in MOEA/D.

In dMOPSO, a swarm of N particles $\mathcal{P} = \{x_1, \ldots, x_N\}$ is randomly initialized. Each particle possesses a flight velocity v_i and an age a_i, both of which are initially set to zero. Along the flight circuits, a particle tries to minimize one of the subproblems in which the MOP is decomposed. Each subproblem is defined by a weighted vector λ according to the Penalty Boundary Intersection (PBI) approach, which is stated as [24]:

$$\text{minimize:} \quad g(x|\lambda, z^\star) = d_1 + \theta d_2 \tag{8}$$

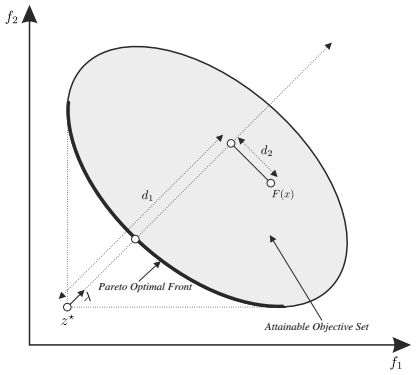

Fig. 2. Illustration of the Penalty Boundary Intersection (PBI) approach.

such that:

$$d_1 = \frac{||(F(x) - z^\star)^T \lambda||}{||\lambda||} \text{ and } d_2 = \left|\left|(F(x) - z^\star) - d_1 \frac{\lambda}{||\lambda||}\right|\right|$$

where $x \in \mathbb{R}^n$, $z^\star = \min\{f_i(x)|x \in \Omega\}$ and $\lambda \in \Lambda$, being Λ a well-distributed set of weighted vectors previously defined. In this way, a Pareto optimal point is reached by minimizing a subproblem defined by the weighted vector λ. Fig. 2 shows the illustration of the PBI approach.

At each cycle, dMOPSO tries to find the best solution to each subproblem. Thus, the *global best* set ($\mathcal{G}_{best}$) is defined in a natural way by storing the solutions that minimize each subproblem and these solutions are identified at each cycle. The *personal best* $x_{pb,i}$ of the i^{th} particle, represents the best solution provided by the particle to the i^{th} subproblem. Since, at the beginning, a particle does not have a previous movement, the best personal position is initialized with the same position as the particle, i.e., $x_{pb,i} = x_i$.

Once the global best set has been defined, the velocity and the position of each particle are updated according to the traditional PSO flight equations:

$$\begin{array}{rcl} v_i^{t+1} & = & wv_i^t + c_1 r_1 (x_{pb,i} - x_t^t) + c_2 r_2 (x_{gb,i} - x_i^t) \\ x_i^{t+1} & = & x_i^t + v_i^{t+1} \end{array} \tag{9}$$

where $w \geq 0$, $c_1, c_2 \geq 0$, $r_1, r_2 \in (0, 1)$, $v_i, x_{pb,i}$ and $x_{gb,i}$ represent the velocity, the personal best and the global best position for the i^{th} particle, respectively.

In dMOPSO, a reinitialization mechanism based on the age of each particle is employed. This mechanism provides

diversity along the flight circuits. When a particle does not improve its personal position in a flight cycle, then the particle increases (by one) its age. On the other hand, if a particle exceeds a certain age threshold (T_a), the particle (including, its velocity, its age and its personal best) is reinitialized according to the following equation:

$$x_i^{t+1}(j) = N\left(\frac{x_{gb,i}(j) - x_{pb,i}(j)}{2}, |x_{gb,i}(j) - x_{pb,i}(j)|\right) \quad (10)$$

where $N(m, \sigma)$ represents a random number using a normal distribution with mean m and sigma σ. As in [23], in our experiments we use $T_a = 2$.

The solutions contained in $\mathcal{G}_{best}$ at the final generation, are reported as an approximation to the Pareto set. For a detailed description of dMOPSO, the interested reader is referred to [23].

IV. Experimental Study

In order to assess the performance of dMOPSO, we compared its results with respect to those generated by the Nondominated Sorting Genetic Algorithm II (NSGA-II) [6] and the Multi-Objective Particle Swarm Optimizer based on Decomposition (MOPSO/D) [18].

A. Performance Measures

For comparing results, we adopted the performance measures described next.

1) R2 Indicator (I_{R2}): The R2 indicator (I_{R2}) proposed in [9] quantifies the distance between the nondominated set or a reference set R and an approximation of the nondominated set A given by an algorithm. Mathematically, it can be expressed as:

$$I_{R2}(A) = \frac{\sum_{\lambda \in \Lambda} u^*(\lambda, R)}{|\Lambda|} \quad (11)$$

where R is a reference set, u^* is the maximum value reached by the utility function u with the weight vector λ, on an approximation set A, i.e., $u^* = \max_{y \in A} u_\lambda(y)$. Λ denotes the set of weight vectors $\lambda \in \mathbb{R}^k$.

Here, we employed the augmented Tchebycheff function as the utility function u. For each test problem, the reference vector R was defined by using the minimum values of each objective found by all the algorithms.

2) Hypervolume difference to a reference set ($I_{\bar{H}}$): The Hypervolume (I_H) indicator was proposed by Zitzler [25]. This performance measure is Pareto compliant [26] and quantifies the approximation of nondominated solutions to the Pareto optimal front. The hypervolume corresponds to the non-overlapped volume of all the hypercubes formed by a reference point r (given by the user) and each solution p in the Pareto set approximation A. It is mathematically defined as:

$$I_H(A) = \Lambda\left(\bigcup_{p \in A} \{x | p \prec x \prec r\}\right) \quad (12)$$

where Λ denotes the Lebesgue measure and $r \in \mathbb{R}^k$ denotes a reference vector being dominated by all valid candidate solutions in A.

Here, we consider the hypervolume difference to a reference set R (commonly, the Pareto optimal front), and we will refer to this indicator as $I_{\bar{H}}$, which is defined as:

$$I_{\bar{H}}(A) = I_H(R) - I_H(A)$$

where smaller values correspond to higher quality as opposed to the original Hypervolume indicator $I_H(A)$.

Since we solve a real-world problem, we do not know the Pareto optimal front. Therefore, for each design problem, we executed all the algorithms for a considerably large number of generations, and the union of all the nondominated solutions obtained was used as the reference set R for this performance measure. For computing I_H, the reference vector r was defined by using the maximum values of each objective function found by all the algorithms over all the runs in each test problem.

B. Multi-Objective Evolutionary Approaches

For each design problem, we performed 30 independent runs with each algorithm. Each run was restricted to 700 generations. For each problem, we used a population size $N = 100$. Therefore, we performed 70,000 fitness function evaluations for each test problem.

Since dMOPSO and MOPSO/D are two decomposition-based algorithms, we used the same scalarization function for a fair comparison, i.e., we used the PBI approach with $\theta = 5$. For all the algorithms (dMOPSO, MOPSO/D and NSGA-II), the parameters were set as the best suited parametric set-up chosen with guidelines from their respective references, see [6, 18, 23]. Since the solutions obtained for each MOEA are not always nondominated, we extracted the best compromise solutions by using the fuzzy membership function based method outlined in [1].

As we mentioned before, the performance of each MOEA was evaluated using the two performance measures previously defined (I_{R2} and $I_{\bar{H}}$). The results are summarized in Tables I, III and V. Each table displays the best, the worst, the average value, as well as the standard deviation of each performance measure, for each test instance. For an easier interpretation, the best results are presented in **boldface** for each performance measure and test problem adopted.

C. Single-Objective Evolutionary Approaches

The individual minima found by each MOEA, i.e., the minimum value reached at each objective function (f_{SLL} and f_{NC}), were compared with respect to those achieved by two single-objective bio-inspired algorithms: a standard Particle Swarm Optimizer (PSO) [11] and an elitist Genetic Algorithm (GA) [8]. For each design problem, we performed 30 independent runs with each single-objective evolutionary approach. Both algorithms were tested using a population size of 100 individuals. As in the multi-objective evolutionary approaches, each run was restricted 70,000 fitness function evaluations (i.e., 700 generations). However, since

we used the single-objective evolutionary approaches for minimizing separately each objective function, we divided the computational cost for each objective, i.e., we employed 350 generations (35,000 fitness function evaluations) for each one.

The PSO algorithm was tested using the traditional inertia equations. The inertia weight w was set linearly decreasing from 0.9 to 0.4. The flight constraints c_1 and c_2 were set in 2. The GA was implemented using a roulette-wheel selection mechanism, one-point crossover and an adaptive feasible mutation operator [13].

The results obtained by each algorithm are reported in Tables II, IV and VI. Each table displays the individual minima and the directivity (in decibels (dB)) obtained by each algorithm for each test problem. The best result for each adopted test problem is presented in **boldface**.

D. Test Problems and Numerical Results

In our study, we compared the performance of the above mentioned MOEAs in three different test problems. In the following, we describe these design problems and their corresponding numerical results are also presented.

1) Example 1: In the first example we have designed a 22-element array having minimum SLL in bands [0°, 82°] and [98°, 180°] with one null in the direction 81°.

Table I provides the results achieved by the multi-objective evolutionary approaches (i.e., dMOPSO, MOPSO/D and NSGA-II) with the adopted performance measures (I_{R2} and $I_{\bar{H}}$). From this table, it is possible to see that the best values for both indicators are obtained by dMOPSO. That means that dMOPSO obtained a better approximation to the Pareto optimal front than MOPSO/D and NSGA-II. These results are validated in Fig. 3, where we show the bi-dimensional Pareto front obtained by all the MOEAs. The figure clearly indicates that by using dMOPSO, it is possible to achieve better trade-off solutions between the two conflicting objectives, namely f_{SLL} and f_{NC}. In Table II, we have provided the individual minima values and the value of directivity for the linear antenna array obtained by the considered single-objective evolutionary algorithms (i.e., PSO and GA). From this table, we can see clearly that the individual minima obtained by dMOPSO is considerably better than those obtained by the single-objective evolutionary approaches. Finally, Fig. 4 plots the normalized power (in dB) versus the elevation angle (in degrees) for all the algorithms over the design corresponding to Example 1.

2) Example 2: In the second example we have increased the number of elements of the array thereby considering a 26-element array having minimum SLL in bands [0°,82°] and [98°, 180°] which has one null in the direction 20°.

In Table III, the performance measures adopted for the comparison of the MOEAs are reported. For both, the I_{R2} and the $I_{\bar{H}}$ indicators, the best values were obtained by dMOPSO. Fig. 5 shows the bi-objective Pareto front obtained by the MOEAs tested here. From this figure, it is possible to see that dMOPSO achieved a better approximation to the Pareto optimal front than the two other MOEAs, although the

TABLE I
BEST, WORST, MEAN AND STANDARD DEVIATIONS OF THE PERFORMANCES MEASURES (I_{R2} AND $I_{\bar{H}}$) ACHIEVED BY EACH MOEA FOR THE EXAMPLE 1

Metric	Value Type	MOPSO/D	NSGA-II	dMOPSO
I_{R2}	*Best*	5.76E-007	4.36E-005	**1.72E-007**
	Worst	7.66E-005	8.72E-004	**6.63E-005**
	Mean	3.86E-005	1.87E-004	**1.65E-005**
	Std. Dev	1.65E-005	5.83E-005	**1.84E-005**
$I_{\bar{H}}$	*Best*	5.87E-006	4.87E-005	**3.28E-006**
	Worst	1.54E-004	7.54E-004	**9.78E-005**
	Mean	8.20E-005	2.87E-004	**6.62E-005**
	Std. Dev	4.29E-005	9.87E-005	**2.68E-005**

TABLE II
INDIVIDUAL MINIMA AND DIRECTIVITY ACHIEVED BY EACH ALGORITHM FOR THE EXAMPLE 1

Algorithms	f_{SSL}	f_{NC}	*Directivity (dB)*
dMOPSO	**0.1056**	**0.0231**	17.587
NSGA-II	0.1672	0.0476	17.282
MOPSO/D	0.1352	0.0532	17.354
GA	0.1852	0.1054	16.192
PSO	0.1762	0.0976	16.823

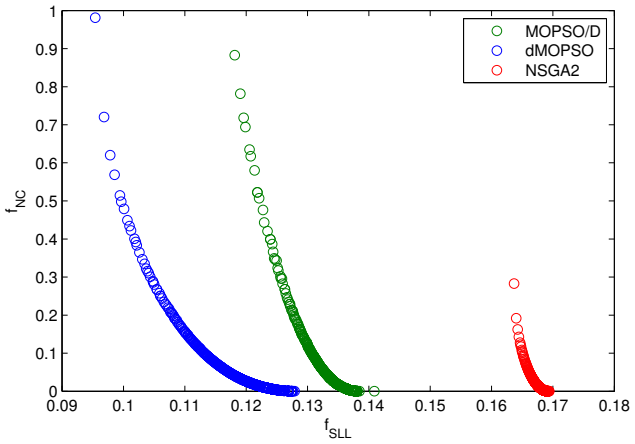

Fig. 3. Best solutions obtained by dMOPSO, MOPSO/D and NSGA-II for the Example 1

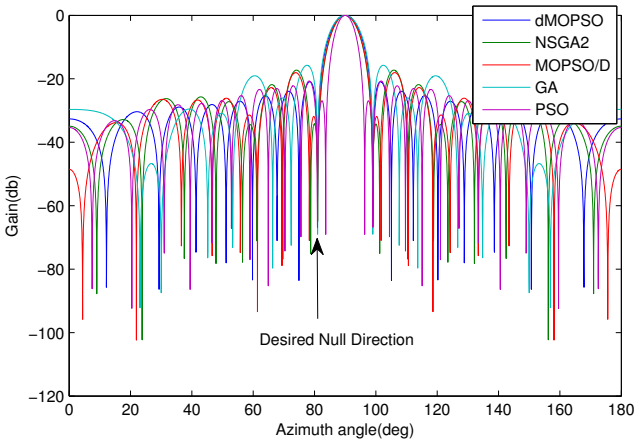

Fig. 4. Array patterns obtained for the Example 1

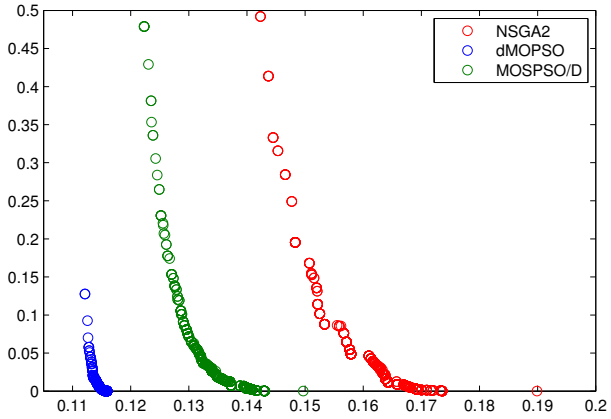

Fig. 5. Best solutions obtained by dMOPSO, MOPSO/D and NSGA-II for the Example 2

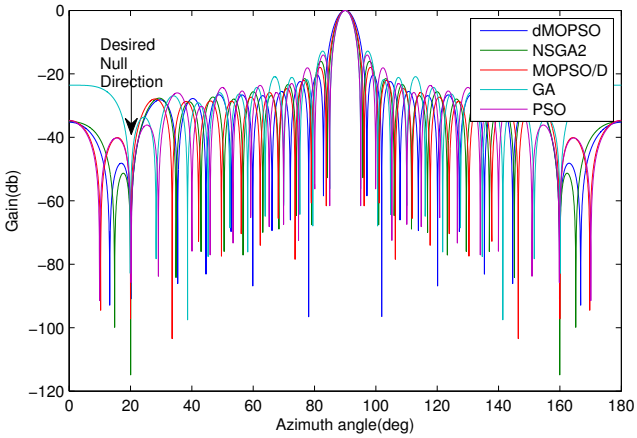

Fig. 6. Array patterns obtained for the Example 2

distribution was not better. However, a better distribution of solutions is relevant only when there is a good approximation to the Pareto front. In Table II, we can see that the individual minima values obtained by dMOPSO are better than those obtained by the single-objective evolutionary approaches. Fig. 6 shows the normalized power versus elevation angle plot for all the algorithms over the design corresponding to Example 2.

TABLE III
BEST, WORST, MEAN AND STANDARD DEVIATIONS OF THE PERFORMANCES MEASURES (I_{R2} AND $I_{\bar{H}}$) ACHIEVED BY EACH MOEA FOR THE EXAMPLE 2

Metric	Value Type	MOPSO/D	NSGA-II	dMOPSO
I_{R2}	*Best*	6.83E-007	5.75E-006	**3.57E-007**
	Worst	2.63E-004	8.03E-004	**9.02E-005**
	Mean	5.98E-005	1.76E-004	**3.10E-005**
	Std. Dev	3.82E-004	1.65E-004	**8.35E-005**
$I_{\bar{H}}$	*Best*	5.20E-005	1.07E-004	**2.66E-005**
	Worst	8.13E-004	3.76E-003	**5.67E-004**
	Mean	4.98E-004	9.24E-004	**1.65E-004**
	Std. Dev	2.63E-004	5.83E-004	**3.76E-004**

TABLE IV
INDIVIDUAL MINIMA AND DIRECTIVITY ACHIEVED BY EACH ALGORITHM FOR THE EXAMPLE 2

Algorithms	f_{SSL}	f_{NC}	*Directivity (dB)*
dMOPSO	**0.1130**	**0.0012**	17.9230
NSGA-II	0.1575	0.0543	17.7540
MOPSO/D	0.1334	0.0234	17.8320
GA	0.1865	0.0965	16.0030
PSO	0.1623	0.0887	16.7240

3) Example 3: In the third example, we consider a 26-element array having minimum SLL in bands [0°, 82°] and [98°, 180°] which has two nulls in the direction 12°and 60°.

For this design instance, Table V shows the results obtained by the MOEAs. The best values for both indicators (I_{R2} and $I_{\bar{H}}$), were obtained by dMOPSO. In Fig. 7, the bi-objective Pareto front achieved by the MOEAs is presented. As it is possible to see, dMOPSO achieved a better approximation to the Pareto optimal front than the other MOEAs. In Table VI, the individual minima values are reported. From this table, we can see that dMOPSO not only obtained better results in terms of the indicators adopted here, but also obtained individual minima that outperformed those obtained by the single-objective evolutionary approaches. Finally, Fig. 8 shows the normalized power versus elevation angle plot for all the algorithms over the design corresponding to Example 3.

TABLE V
BEST, WORST, MEAN AND STANDARD DEVIATIONS OF THE PERFORMANCES MEASURES (I_{R2} AND $I_{\bar{H}}$) ACHIEVED BY EACH MOEA FOR THE EXAMPLE 3

	Value Type	MOPSO/D	NSGA-II	dMOPSO
I_{R2}	*Best*	6.86E-007	5.05E-006	**3.01E-007**
	Worst	8.13E-005	4.83E-004	**7.75E-005**
	Mean	2.06E-005	3.45E-005	**1.01E-005**
	Std. Dev	8.63E-005	9.27E-005	**5.82E-005**
$I_{\bar{H}}$	*Best*	1.76E-005	8.20E-005	**1.03E-005**
	Worst	6.43E-005	6.65E-004	**5.33E-005**
	Mean	3.97E-005	2.47E-004	**2.06E-005**
	Std. Dev	4.54E-006	5.92E-006	**1.87E-006**

TABLE VI
INDIVIDUAL MINIMA AND DIRECTIVITY ACHIEVED BY EACH ALGORITHM FOR THE EXAMPLE 3

Algorithms	f_{SSL}	f_{NC}	*Directivity (dB)*
dMOPSO	**0.1452**	**0.0154**	17.8240
NSGA-II	0.1593	0.0197	17.6920
MOPSO/D	0.1557	0.0203	17.5630
GA	0.1825	0.0431	17.0320
PSO	0.1733	0.0511	17.2130

V. DISCUSSION OF RESULTS

According to results presented in Tables I to VI, dMOPSO has clearly shown its superiority in terms of the performance measures considered here. These tables provide a quantitative assessment of the performance of dMOPSO in terms of

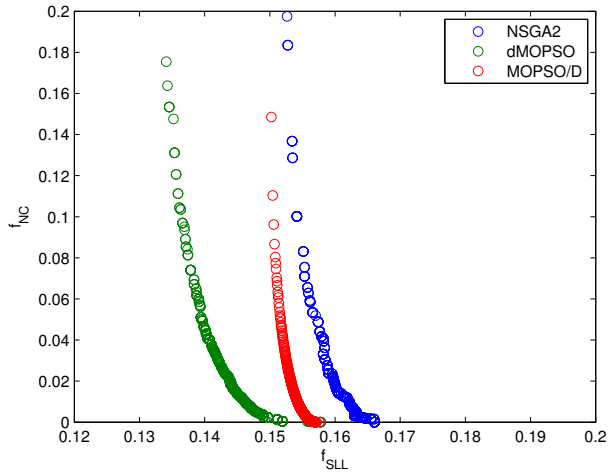

Fig. 7. Best solutions obtained by dMOPSO, MOPSO/D and NSGA-II for the Example 3

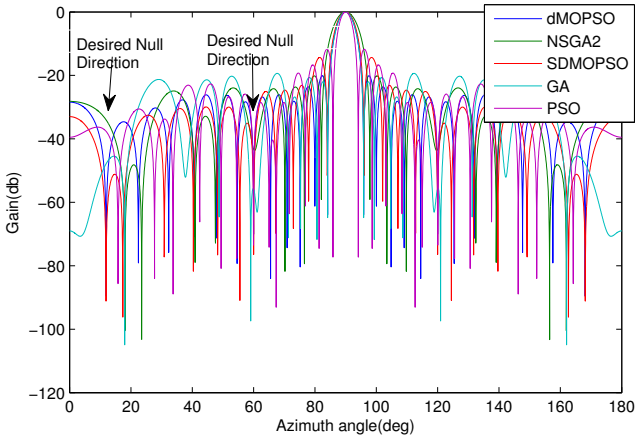

Fig. 8. Array patterns obtained for the Example 3

the I_{R2} and $I_{\bar{H}}$ indicators. That means that the solutions obtained by dMOPSO constitute a better approximation to the Pareto optimal front than the solutions obtained by either MOPSO/D or NSGA-II. As it is possible to see in Tables II, IV and VI, dMOPSO also reached better values for the individual minima reported by the two single-objective evolutionary approaches. It is worth noting that dMOPSO was not the only MOEA capable to obtaining good individual minima. In fact, the other two MOEAs also achieved better individual minima than those obtained by the single-objective evolutionary approaches. We believe that this good performance of the MOEAs evaluated in our experimental study can be attributed to their diversity maintenance mechanism, which allows a better exploration of different regions of the search space than that provided by a single-objective optimizer. In the case of NSGA-II, this diversity is provided by its crowded-comparison operator [6], which promotes the exploration of regions of the Pareto front which contain isolated solutions. In the case of MOEAs based on decomposition (i.e., dMOPSO and MOPSO/D), the algorithms try to minimize different problems defined by a well distributed set of weighted vectors and the PBI approach. In other words, the solutions are guided by each weighted vector, and the parameter θ enforces the search in a specific direction, providing diversity in the search. The single-objective evolutionary algorithms adopted don't have a similar mechanism to maintain diversity and are simply guided by the aim of improving, as much as possible, the best solution obtained so far.

VI. Conclusions and Future Work

In this work, we have incorporated an additional objective function (called the Maximum Side Lobe Level (MSLL)) into the linear antenna array design problem which has been formulated as a bi-objective optimization problem. The two objectives considered here, are optimized simultaneously in a multi-objective framework. Then, a MOEA is adopted as our search engine. Our results indicate that MOEAs provide greater flexibility in the linear antenna array design problem, by producing a set of solutions from which the designer can choose the most preferred according to his/her own particular preferences. In our study, we adopted one of the recently developed variants of PSO for multi-objective optimization called dMOPSO, which was developed by two of the co-authors of this paper. The adopted algorithm has been tested in three different instances of the design problem of our interest. The results obtained by dMOPSO were compared with respect to those obtained by two state-of-the-art MOEAs, namely NSGA-II and MOPSO/D. Additionally, the individual minima obtained were compared with respect to those attained by two single-objective algorithms (a PSO approach and an elitist GA).

The results indicate that dMOPSO outperforms all the other approaches with respect to which it was compared (including the single-objective techniques). In fact, all the MOEAs adopted were able to outperform the individual minima obtained by the single-objective optimizers used in our study, giving evidence of the benefits of the more diversified search that they perform.

As part of our future work, we are interested in having more control of the array pattern by using dMOPSO for optimizing the excitation amplitude and phase of each element in the array. We also aim to investigate the use of dMOPSO in other (more complex) antenna design problems which are currently modeled as single-objective optimization problems. Additionally, we are also interested in hybridizing dMOPSO with direct search methods available in the mathematical programming literature (e.g., Hooke-Jeeves [10] or Nelder-Mead [16] method) aiming to improve its performance. The idea is to use the evolutionary strategy to explore the search space as a whole and the mathematical programming method to exploit promissory regions within it (acting as a local search engine).

ACKNOWLEDGMENTS

The second author acknowledges support from CONACyT through a scholarship to pursue graduate studies at the Computer Science Department of CINVESTAV-IPN. The third author gratefully acknowledges support from CONACyT project no. 103570.

REFERENCES

[1] M. A. Abido. A Niched Pareto Genetic Algorithm for multiobjective environmental/economic dispatch. *International Journal of Electrical Power & Energy Systems*, 25(2):97–105, February 2003.

[2] F. Ares-Pena, J. Rodriguez-Gonzalez, E. Villanueva-Lopez, and S. Rengarajan. Genetic algorithms in the design and optimization of antenna array patterns. *IEEE Transactions on Antennas and Propagation*, 47(3):506–510, March 1999.

[3] Y. Cengiz and H. Tokat. Linear antenna array design with use of genetic, memetic and tabu search optimization algorithms. *Progress In Electromagnetics Research C*, 1:63–72, 2008.

[4] S. Chandran. *Adaptive Antenna Arrays: Trends and Applications (Signals and Communication Technology)*. Springer Verlag, 2004.

[5] A. Chowdhury, R. Giri, A. Ghosh, S. Das, A. Abraham, and V. Snasel. Linear antenna array synthesis using fitness-adaptive differential evolution algorithm. In *2010 IEEE Congress on Evolutionary Computation (CEC'2010)*, pages 1–8, july 2010.

[6] K. Deb, A. Pratap, S. Agarwal, and T. Meyarivan. A Fast and Elitist Multiobjective Genetic Algorithm: NSGA–II. *IEEE Transactions on Evolutionary Computation*, 6(2):182–197, April 2002.

[7] L. Godara. *Handbook of Antennas in Wireless Communications*. CRC Press, Inc., Boca Raton, FL, USA, 2001.

[8] D. E. Goldberg. *Genetic Algorithms in Search, Optimization and Machine Learning*. Addison-Wesley Longman Publishing Co., Inc., Boston, MA, USA, 1989.

[9] M. P. Hansen and A. Jaszkiewicz. Evaluating the quality of approximations to the non-dominated set. Technical report, Institute of Mathematical Modeling, Technical University of Denmark, 1998.

[10] R. Hooke and T. A. Jeeves. "direct search" solution of numerical and statistical problems. *J. ACM*, 8(2):212–229, 1961.

[11] J. Kennedy and R. C. Eberhart. Particle swarm optimization. In *Proceedings of the IEEE International Conference on Neural Networks*, pages 1942–1948, 1995.

[12] M. Khodier and C. Christodoulou. Linear array geometry synthesis with minimum sidelobe level and null control using particle swarm optimization. *IEEE Transactions on Antennas and Propagation*, 53(8):2674–2679, August 2005.

[13] R. Kumar. System and method for the use of an adaptive mutation operator in genetic algorithms, February 2010. Patent No US 7,660,773.

[14] K. Miettinen. *Nonlinear Multiobjective Optimization*, volume 12 of *International Series in Operations Research and Management Science*. Kluwer Academic Publishers, Dordrecht, 1999.

[15] N. A. Moubayed, A. Petrovski, and J. A. W. McCall. A novel smart multi-objective particle swarm optimisation using decomposition. In *PPSN (2)*, pages 1–10, 2010.

[16] J. A. Nelder and R. Mead. A Simplex Method for Function Minimization. *The Computer Journal*, 7:308–313, 1965.

[17] S. Pal, B. Qu, S. Das, and P. Suganthan. Optimal synthesis of linear antenna arrays with multi-objective differential evolution. *Progress In Electromagnetics Research B*, 21:87–111, 2010.

[18] W. Peng and Q. Zhang. A decomposition-based multi-objective particle swarm optimization algorithm for continuous optimization problems. In *IEEE International Conference on Granular Computing, 2008. GrC 2008*, pages 534–537, 2008.

[19] Y. Rahmat-Samii and E. Michielssen, editors. *Electromagnetic Optimization by Genetic Algorithms*. John Wiley & Sons, Inc., New York, NY, USA, 1st edition, 1999.

[20] G. V. Tsoulos. *Adaptive Antennas for Wireless Communications*. Wiley-IEEE Press, Boca Raton, FL, USA, 2001.

[21] A. Udina, N. Martin, and L. Jain. Linear antenna array optimisation by genetic means. In *Knowledge-Based Intelligent Information Engineering Systems, 1999. Third International Conference*, pages 505–508, December 1999.

[22] W.-C. Weng, F. Yang, and A. Elsherbeni. Linear antenna array synthesis using taguchi's method: A novel optimization technique in electromagnetics. *IEEE Transactions on Antennas and Propagation*, 55(3):723–730, March 2007.

[23] S. Zapotecas Martínez and C. A. Coello Coello. A Multi-objective Particle Swarm Optimizer Based on Decomposition. In *GECCO'2011*, pages 69–76, Dublin, Ireland, July 2011. ACM.

[24] Q. Zhang and H. Li. MOEA/D: A Multiobjective Evolutionary Algorithm Based on Decomposition. *IEEE Transactions on Evolutionary Computation*, 11(6):712–731, December 2007.

[25] E. Zitzler and L. Thiele. Multiobjective Optimization Using Evolutionary Algorithms – A Comparative Case Study. In A. E. Eiben, editor, *PPSN V*, pages 292–301, Amsterdam, September 1998. Springer-Verlag.

[26] E. Zitzler, L. Thiele, M. Laumanns, C. M. Fonseca, and V. G. da Fonseca. Performance Assessment of Multiobjective Optimizers: An Analysis and Review. *IEEE Transactions on Evolutionary Computation*, 7(2):117–132, April 2003.